

Two-dimensional hybrid simulations of the oblique electromagnetic alpha/proton instability in the solar wind

Quanming Lu,^{1,a)} Aimin Du,^{1,2} and Xing Li^{1,3}

¹*School of Earth and Space Sciences, University of Science and Technology of China, Hefei 230026, China*

²*Institute of Geology and Geophysics, Chinese Academy of Sciences, Beijing 100029, China*

³*Institute of Mathematics and Physics, Aberystwyth University, Aberystwyth SY23 3BZ, United Kingdom*

(Received 20 January 2009; accepted 18 March 2009; published online 21 April 2009)

In the solar wind, alpha particles are observed to flow faster than the core protons. In this paper, two-dimensional hybrid simulations are performed to investigate the nonlinear evolution of oblique Alfvén waves excited by an alpha/proton beam instability in a low beta plasma. The propagation angles of the excited waves are within a finite range suggesting the generation of oblique Alfvén waves. During the nonlinear evolution, both the wave numbers and frequencies of the waves drift to smaller values, and the propagation angles decrease. At the same time, the propagation angle of the dominant mode also changes. Eventually the plasma system reaches a marginally stable state according to linear theory. © 2009 American Institute of Physics. [DOI: 10.1063/1.3116651]

I. INTRODUCTION

In situ measurements have shown that there exists a variety of ion beams in the fast solar wind. The proton velocity distributions in the solar wind are observed to have two peaks, which can be considered to consist of two components (the core and beam protons) with an average relative drift velocity U_{pp} (where $1 < U_{pp}/V_A \leq 2$ and V_A is the local Alfvén speed) parallel to the background magnetic field \mathbf{B}_0 .^{1,2} There is also a relative streaming between minor ions such as alpha particles and the core protons.^{3–5} In general, the alpha particles flow faster than the core protons. The average drift velocity is around the local Alfvén speed and its direction is parallel to the background magnetic field.

Both linear Vlasov theory and hybrid simulations have shown that such ion beams are unstable to two kinds of electromagnetic waves under typical conditions in the fast solar wind, and they are magnetosonic and Alfvén instabilities.^{6,7} The right-hand polarized magnetosonic waves with the maximum growth rate along the background magnetic field are more likely to grow at $\beta_{\parallel p} \geq 1$ (where $\beta_{\parallel p} = 8\pi n_p k_B T_p / B_0^2$ is the parallel proton plasma beta).^{8,9} The left-hand polarized Alfvén waves are likely to propagate obliquely to the background magnetic field, and they tend to be excited at $\beta_{\parallel p} \ll 1$.¹⁰ The effects of the temperature anisotropies (the ratio of perpendicular temperature to parallel temperature) of the core protons and beam particles on the beam instabilities have also been studied, and such anisotropies can be explained by the scattering of the intrinsic ion cyclotron waves in the fast solar wind.^{11,12} Linear Vlasov theory found that the increase in the core/beam temperature anisotropy can reduce the growth rates of both the magnetosonic and Alfvén instabilities.^{6,13} This has been verified by one-dimensional (1D) hybrid simulations.^{14,15} In this paper, with two-dimensional (2D) hybrid simulations we investigate the nonlinear evolution of the oblique left-hand polarized Alfvén waves excited by an alpha particle beam.

In hybrid simulations, ions are treated kinetically and electrons are considered as a massless fluid.¹⁶ The particles are advanced according to the well-known Boris algorithm while the electromagnetic fields are calculated with an implicit algorithm.¹⁷ The plasma is presumed to be collisionless, homogeneous, and magnetized, and it consists of two ion components (protons and alpha particles) and the massless electron fluid. Their number densities are n_p , n_α , and n_e , respectively. Initially, both alpha particles and protons satisfy bi-Maxwellian velocity distribution and they have the same parallel thermal speed. The alpha particles have a drift speed U_{0ap} along the background magnetic field \mathbf{B}_0 . The temperature anisotropies for protons and alpha particles are $T_{\perp p}/T_{\parallel p} = 2.0$ and $T_{\perp \alpha}/T_{\parallel \alpha} = 0.5$, respectively. The electrons are isotropic and their temperature is a quarter of the proton parallel temperature, similar to that in the fast solar wind.

II. SIMULATION MODEL

A 2D hybrid simulation model with periodic boundary conditions is used in this paper. In the model, units of space and time are c/ω_{pp} (where c/ω_{pp} is the proton inertial length, c is the speed of light, and ω_{pp} is the proton plasma frequency based on total number density $n_0 = n_p + n_\alpha$) and Ω_p^{-1} (where $\Omega_p = eB_0/m_p$ is the proton gyrofrequency), respectively. We choose $n_\alpha/n_e = 0.05$, and the initial drift speed between alpha particles and protons U_{0ap} is set at $1.55V_A$. The direction of the drift is parallel to the background magnetic field $\mathbf{B}_0 = B_0 \hat{x}$. The simulations are performed in the center-of-mass frame, where charge neutrality ($\sum_j e_j n_j = 0$, where j denotes the species of particles) and the zero current condition ($\sum_j e_j n_j V_{0j} = 0$) are imposed at $t=0$. The number of grid cells is $n_x \times n_y = 512 \times 256$ and the grid sizes are $\Delta x = 0.8c/\omega_{pp}$ and $\Delta y = 0.8c/\omega_{pp}$ with 100 particles per cell for each ion component. The time step is $\Omega_p \Delta t = 0.025$. For comparison, a 1D hybrid simulation with the periodic boundary conditions is also performed, and the parameters are the

^{a)}Electronic mail: qmlu@ustc.edu.cn.

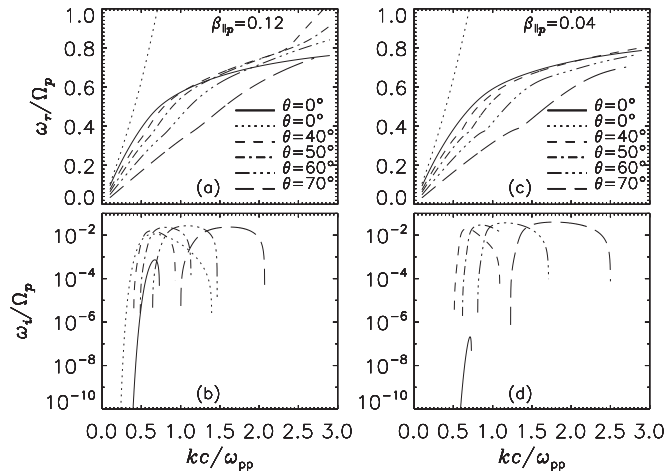


FIG. 1. Dispersion relation (top panels) and growth rate (bottom panels) of left-handed parallel propagating shear Alfvén mode (solid), right-handed parallel propagating magnetosonic mode (dotted), and oblique Alfvén mode at different propagating angles 40° , 50° , 60° , and 70° . Left and right panels are for the case of different initial proton parallel beta values of 0.12 and 0.04, respectively.

same as the 2D model. The number of grid is $n_x=512$ and grid size is $\Delta x=0.8c/\omega_{pp}$ with 300 particles for each ion component. The angle between the background magnetic field and the x direction is 45° , which assumes the propagation angle of the waves to be 45° .

III. LINEAR THEORY AND SIMULATION RESULTS

Both parallel magnetosonic and oblique Alfvén instabilities may be excited by an alpha/proton drift. We choose two different values of the parallel proton plasma beta: $\beta_{||p}=0.12$ and 0.04. In such situations, the oblique Alfvén waves have the highest growth rate.⁶ The chosen parallel proton plasma beta values may represent solar wind conditions from the corona base to 0.3 AU,¹⁸ where *in situ* measurements are not available.

Figure 1 shows the dispersion relation and growth rate of oblique Alfvén waves at different propagation angles. For comparison, parallel propagating shear Alfvén mode and magnetosonic mode are also displayed. At $\beta_{||p}=0.04$, the parallel propagating shear Alfvén mode has very small growth rates while the parallel magnetosonic mode is very stable. On the other hand, at a higher beta the growth rates of the two parallel models become much larger. However they are still significantly smaller than the maximum growth rate of the oblique Alfvén mode at $\beta_{||p}=0.12$. For $\beta_{||p}=0.12$, the dispersion relation changes its trend at roughly $kc/\omega_{pp} \approx 2.3$ at propagation angle of 40° , representing a mode exchange between the shear Alfvén mode and magnetosonic mode.¹⁹

Figure 2 shows the time evolution of (a) the amplitude of the fluctuating magnetic field $\delta B^2/B_0^2$, (b) the relative drift speed between alpha and proton particles U_{ap}/V_A , (c) the temperature anisotropy of alpha particles $T_{\perp\alpha}/T_{||\alpha}$, and (d) the temperature anisotropy of protons $T_{\perp p}/T_{||p}$ for $\beta_{||p}=0.12$.

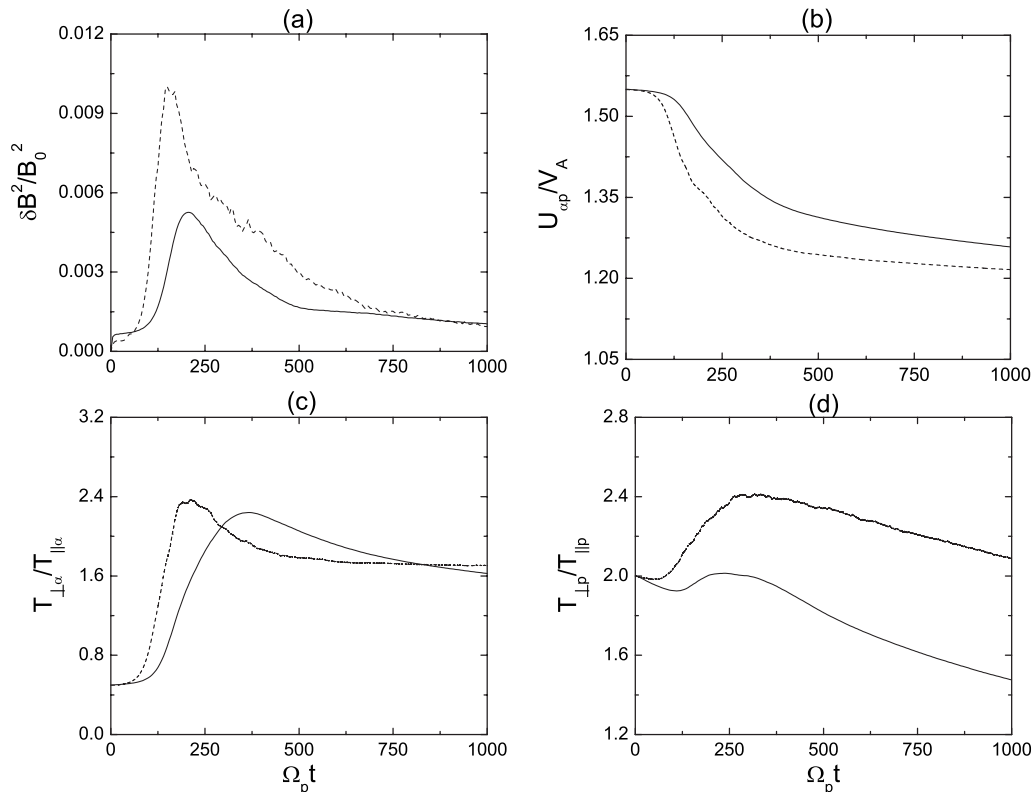


FIG. 2. The time evolution of (a) the amplitude of the fluctuating magnetic field $\delta B^2/B_0^2$, (b) the relative drift speed between alpha and proton particles U_{ap}/V_A , (c) the temperature anisotropy of alpha particles $T_{\perp\alpha}/T_{||\alpha}$, and (d) the temperature anisotropy of proton particles $T_{\perp p}/T_{||p}$ for $\beta_{||p}=0.12$ in 2D (solid) and 1D (dotted) simulations.

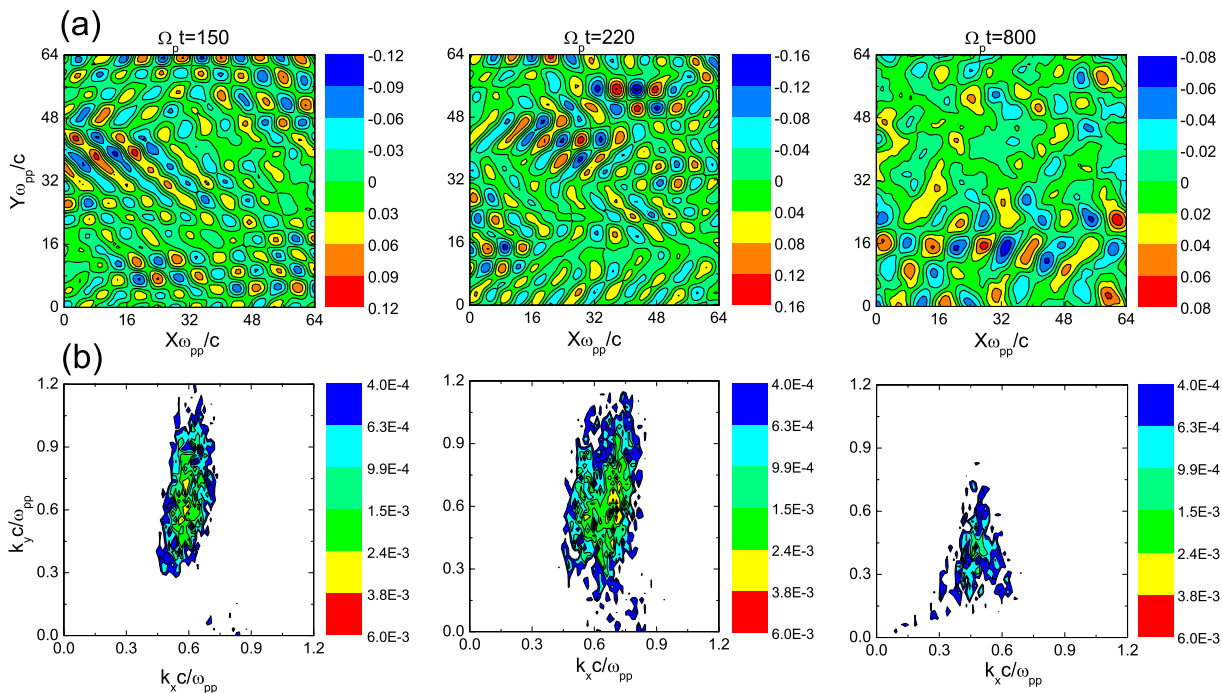


FIG. 3. (Color online) (a) The contour plot of the fluctuating magnetic field along the z direction B_z/B_0 and (b) the characteristics of k_x-k_y diagram obtained from the FFT transforming B_z/B_0 at different times for $\beta_{\parallel p}=0.12$.

We calculate the parallel and perpendicular temperatures using the following procedure: we first calculate the parallel temperature $T_{\parallel j}=m_j/k_B(\langle v_x-\langle v_x \rangle \rangle^2)$ and the perpendicular temperature $T_{\perp j}=m_j/2k_B(\langle v_y-\langle v_y \rangle \rangle^2+\langle v_z-\langle v_z \rangle \rangle^2)$ in every grid (the bracket $\langle \cdot \rangle$ denotes an average over a grid cell), and then the temperatures are averaged over all grids. In this way, we can eliminate the effects of the average velocity at each location on the thermal temperature. In 2D simulation, the waves begin to be excited at $\Omega_p t \approx 100$, and they saturate at $\Omega_p t \approx 200$ with the amplitude $\delta B^2/B_0^2 \approx 0.0053$. Then the amplitude decreases gradually until the quasiequilibrium stage (from $\Omega_p t \approx 500$) with the amplitude $\delta B^2/B_0^2 \approx 0.001$. With the excitation of the oblique Alfvén waves, the relative drift speed between alpha and proton particles U_{ap}/V_A decreases, while the temperature anisotropies of alpha and proton particles ($T_{\perp \alpha}/T_{\parallel \alpha}$ and $T_{\perp p}/T_{\parallel p}$) increase. The temperature anisotropies attain their maximum values slightly after the amplitude of the excited waves attains their maximum, and then they begin to decrease during the nonlinear evolution. At the quasiequilibrium stage, U_{ap}/V_A , $T_{\perp \alpha}/T_{\parallel \alpha}$, and $T_{\perp p}/T_{\parallel p}$ are 1.26, 1.6, and 1.5, respectively. Compared with 2D simulation, the evolution of waves is similar in 1D simulation. However, the waves at the saturation stage have larger amplitude, and the alpha beam is decelerated more efficiently. At the quasiequilibrium stage, U_{ap}/V_A , $T_{\perp \alpha}/T_{\parallel \alpha}$, and $T_{\perp p}/T_{\parallel p}$ are 1.22, 1.7, and 2.1, respectively.

Figure 3 shows (a) the contour plot of the fluctuating magnetic field along the z direction B_z/B_0 and (b) the characteristics of k_x-k_y diagram obtained from the fast Fourier transform (FFT) transforming of B_z/B_0 at different times for $\beta_{\parallel p}=0.12$ in 2D simulation. The obliquely propagating Alfvén waves can be obviously found. At $\Omega_p t=150$, the dominant $(k_x \omega_{pp}/c, k_y \omega_{pp}/c)$ (at that point, the power has the

maximum value) is at about (0.6, 0.6). At $\Omega_p t=220$ and 800, the dominant $(k_x \omega_{pp}/c, k_y \omega_{pp}/c)$ is at about (0.7, 0.55) and (0.45, 0.45), respectively. Therefore, both the wave number and frequency of the dominant mode at the quasiequilibrium stage are smaller than that at the linear growth stage, and the propagation angle $\theta=\arctan(k_y/k_x)$ of the dominant mode changes in the nonlinear evolution. At the same time, the propagation angle θ has a definite range and it becomes smaller during the nonlinear evolution. At $\Omega_p t=150$, 220, and 800, the ranges of the propagation angle are about from 27° to 60° , 17° to 58° , and 14° to 53° , respectively. It is noted that in this case, there are some quasiparallel propagating waves with $0 < kc/\omega_{pp} < 0.9$. They are very likely magnetosonic waves in accordance with the linear theory results.

Figure 4 shows the time evolution of (a) the amplitude of the fluctuating magnetic field $\delta B^2/B_0^2$, (b) the relative drift speed between alpha and proton particles U_{ap}/V_A , (c) the temperature anisotropy of the alpha particles $T_{\perp \alpha}/T_{\parallel \alpha}$, and (d) the temperature anisotropy of protons $T_{\perp p}/T_{\parallel p}$ for $\beta_{\parallel p}=0.04$. In 2D simulation, waves begin to be excited at $\Omega_p t \approx 75$ and saturate at $\Omega_p t \approx 130$ with the amplitude $\delta B^2/B_0^2 \approx 0.007$. Compared with the case for $\beta_{\parallel p}=0.12$, the linear growth rate of the oblique Alfvén waves is larger, which is consistent with the linear Vlasov theory (see Fig. 1). Then the amplitude begins to decrease and the quasiequilibrium stage is attained at $\Omega_p t \approx 750$ with the amplitude $\delta B^2/B_0^2 \approx 0.0009$, which is almost the same as the case for $\beta_{\parallel p}=0.12$. Similar to the case for $\beta_{\parallel p}=0.12$ with the excitation of the oblique Alfvén waves, the relative drift speed between alpha and proton particles U_{ap}/V_A decreases while the temperature anisotropies of alpha and proton particles ($T_{\perp \alpha}/T_{\parallel \alpha}$ and $T_{\perp p}/T_{\parallel p}$) increase, and the temperature anisotropies attain their maximum values slightly after the

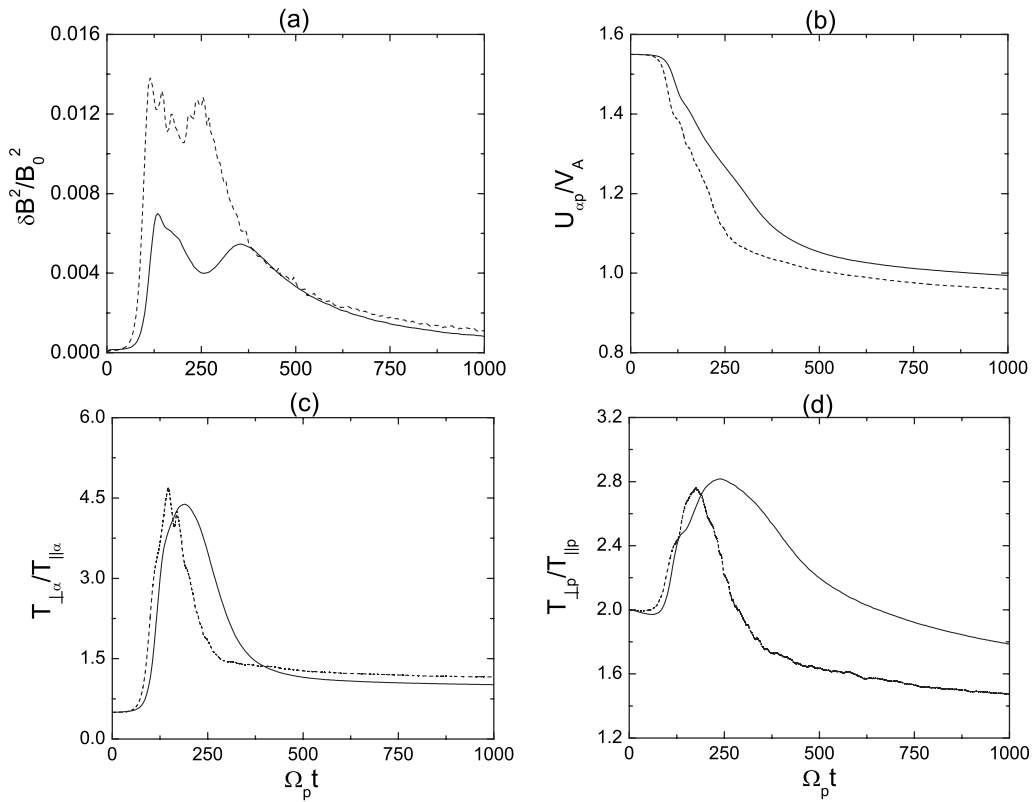


FIG. 4. The time evolution of (a) the amplitude of the fluctuating magnetic field $\delta B^2/B_0^2$, (b) the relative drift speed between alpha and proton particles U_{ap}/V_A , (c) the temperature anisotropy of alpha particles $T_{\perp\alpha}/T_{\parallel\alpha}$, and (d) the temperature anisotropy of proton particles $T_{\perp p}/T_{\parallel p}$ for $\beta_{lp}=0.04$ in 2D (solid) and 1D (dotted) simulations.

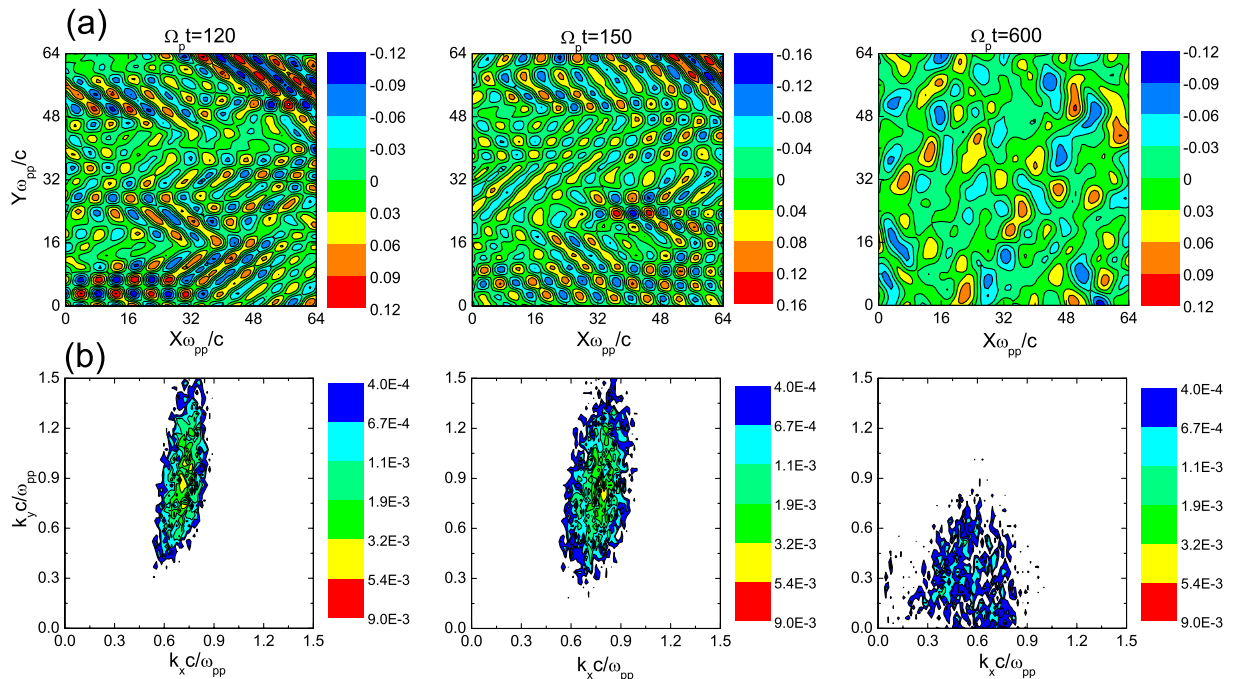


FIG. 5. (Color online) (a) The contour plot of the fluctuating magnetic field along the z direction B_z/B_0 and (b) the characteristics of k_x-k_y diagram obtained from the FFT transforming B_z/B_0 at different times for $\beta_{lp}=0.04$.

amplitude of the excited waves attains their maximum. At the quasiequilibrium stage, $U_{\alpha p}$ is around the local Alfvén speed, $T_{\perp\alpha}/T_{\parallel\alpha}$ and $T_{\perp p}/T_{\parallel p}$ are 1.0 and 1.8, respectively. We can find obvious heating of the proton particles with the excitation of the oblique Alfvén waves. In Figs. 2 and 4, the final nonlinear states are near marginal stability according to linear theory: the growth rate of unstable modes becomes about an order of magnitude smaller than that of the initial states. Similar to the case of $\beta_{\parallel p}=0.12$, in 1D simulation the unstable waves at the saturation stage have larger amplitude, and the alpha beam is decelerated again more efficiently.

Figure 5 shows (a) the contour plot of the fluctuating magnetic field along the z direction B_z/B_0 and (b) the characteristics of k_x-k_y diagram obtained from the FFT transforming B_z/B_0 at different times for $\beta_{\parallel p}=0.04$ in 2D simulation. At $\Omega_p t=120, 150,$ and 600 , the dominant $(k_x\omega_{pp}/c, k_y\omega_{pp}/c)$ is at about $(0.75, 0.82), (0.8, 0.9),$ and $(0.6, 0.6)$. Similar to the case of $\beta_{\parallel p}=0.12$, both the wave numbers and frequencies of the dominant mode at the quasiequilibrium stage are smaller than that at the linear growth stage and its propagation angle θ also changes. At the same time, the range of the propagation angle θ becomes smaller. At $\Omega_p t=150, 220,$ and 800 , the ranges of the propagation angle are about from 30° to $65^\circ, 25^\circ$ to $58^\circ,$ and 0° to $52^\circ,$ respectively.

IV. CONCLUSIONS AND DISCUSSION

In this paper, with 2D dimensional hybrid simulations we investigate the nonlinear evolution of obliquely propagating Alfvén waves excited by an alpha/proton drift. The nonlinear evolution may provide a possible mechanism to decelerate the alpha beam in the solar wind. In a low beta plasma, the oblique Alfvén waves have larger linear growth rate and saturation amplitude, and the relative drift speed between the alpha and proton particles is smaller at the quasiequilibrium stage. The nonlinear evolution of the streaming instability leads to the relaxation of the system. Eventually the nonlinear state is near the marginal stability according to linear theory. During the nonlinear evolution, both the wave numbers and frequencies of the excited waves tend to drift to smaller values. The propagation angles of the waves have a definite range and, in general, decrease during the nonlinear evolution. At the same time, the propagation angle of the dominant mode also changes. Therefore, 1D hybrid simulations, in which the propagation angle of all excited Alfvén modes is fixed at a specific direction, may cause some inaccuracy to study the nonlinear evolution of the oblique alpha/proton instability (as shown in Figs. 2 and 4).

Magnetic field observations in the solar wind have shown that oblique waves have significant power and mag-

netohydrodynamics (MHD) turbulence theory generally favors the generation of oblique waves.²⁰⁻²² The oblique Alfvén waves produced by beam alpha particles in this paper or by other means may be relevant to the heating of the solar wind, an ongoing research topic in solar-terrestrial physics.

It is recognized that 2D hybrid models like ours have their own limitations. Electron Landau damping could be important in low beta plasmas. Such effect can only be dealt with in 2D particle-in-cell (PIC) models.²³

ACKNOWLEDGMENTS

This research was supported by the National Science Foundation of China (NSFC) under Grant Nos. 40725013, 40674093, and 40574063 and Chinese Academy of Sciences under Grant No. KJCX2-YW-N28.

- ¹W. C. Feldman, J. T. Gosling, D. J. McComas, and J. L. Phillips, *J. Geophys. Res.* **98**, 5593, DOI: 10.1029/92JA02260 (1993).
- ²B. Goldstein, M. Neugebauer, L. D. Zhang, and S. P. Gary, *Geophys. Res. Lett.* **27**, 53, DOI: 10.1029/1999GL003637 (2000).
- ³E. Marsch, K. H. Muhlhauser, H. Rosenbauer, R. Schwenn, and F. M. Neubauer, *J. Geophys. Res.* **87**, 35, DOI: 10.1029/JA087iA01p00035 (1982).
- ⁴M. Neugebauer, B. E. Goldstein, S. J. Bame, and W. C. Feldman, *J. Geophys. Res.* **99**, 2505, DOI: 10.1029/93JA02615 (1994).
- ⁵R. Von Steiger, J. Geiss, G. Gloeckler, and A. B. Galvin, *Space Sci. Rev.* **72**, 71 (1995).
- ⁶W. Daughton and S. P. Gary, *J. Geophys. Res.* **103**, 20613, DOI: 10.1029/98JA01385 (1998).
- ⁷W. Daughton, S. P. Gary, and D. Winske, *J. Geophys. Res.* **104**, 4657, DOI: 10.1029/1998JA900105 (1999).
- ⁸S. P. Gary, *Space Sci. Rev.* **56**, 373 (1991).
- ⁹S. P. Gary, L. Yin, D. Winske, and D. B. Reisenfeld, *J. Geophys. Res.* **105**, 20989, DOI: 10.1029/2000JA000049 (2000).
- ¹⁰S. P. Gary, L. Yin, D. Winske, and D. B. Reisenfeld, *Geophys. Res. Lett.* **27**, 1355, DOI: 10.1029/2000GL000019 (2000).
- ¹¹X. Li and S. R. Habbal, *Sol. Phys.* **190**, 485 (1999).
- ¹²Q. M. Lu and S. Wang, *Chin. J. Astron. Astrophys.* **5**, 184 (2005).
- ¹³X. Li and S. R. Habbal, *J. Geophys. Res.* **105**, 7483, DOI: 10.1029/1999JA000259 (2000).
- ¹⁴Q. M. Lu, L. D. Xia, and S. Wang, *J. Geophys. Res.* **111**, A09101, DOI: 10.1029/2006JA011752 (2006).
- ¹⁵J. A. Araneda, A. F. Vinas, and H. F. Astudillo, *J. Geophys. Res.* **107**, 1453, DOI: 10.1029/2002JA009337 (2002).
- ¹⁶D. Winske, *Space Sci. Rev.* **42**, 53 (1985).
- ¹⁷Q. M. Lu and S. Wang, *Geophys. Res. Lett.* **32**, L03111, DOI: 10.1029/2004GL021508 (2005).
- ¹⁸X. Li, S. R. Habbal, J. V. Hollweg, and R. Esser, *J. Geophys. Res.* **104**, 2521, DOI: 10.1029/1998JA900126 (1999).
- ¹⁹X. Li and S. R. Habbal, *J. Geophys. Res.* **106**, 10669, DOI: 10.1029/2000JA000420 (2001).
- ²⁰R. J. Leamon, C. W. Smith, N. F. Ness, and H. K. Wong, *J. Geophys. Res.* **104**, 22331, DOI: 10.1029/1999JA900158 (1999).
- ²¹J. J. Podesta, D. A. Roberts, and M. L. Goldstein, *Astrophys. J.* **664**, 543 (2007).
- ²²G. G. Howes, *Phys. Plasmas* **15**, 055904 (2008).
- ²³L. Yin, D. Winske, W. Daughton, and K. J. Bowers, *Phys. Plasmas* **14**, 062104 (2007).